Spin waves in a doped antiferromagnet

Jun-ichi Igarashi
Max-Planck-Institut für Festkörperforschung, D-7000 Stuttgart 80, Germany
and Department of Physics, Faculty of Science, Osaka University, Toyonaka, Osaka 560, Japan

Peter Fulde
Max-Planck-Institut für Festkörperforschung, D-7000 Stuttgart 80, Germany
(Received 24 October 1991)

Spin waves are studied in the t-J model for low dopant concentrations on the basis of a Green's-function formalism in a slave-fermion Schwinger boson representation. The self-consistent Born approximation is used to calculate the Green's function for holes. Both the coupling of spin waves to electron-hole pair excitations and the scattering of spin waves by holes are taken into account in calculating the Green's function for spin waves. The spin-wave velocity is evaluated for various values of J/t. For small values of J/t, it is found to be strongly renormalized due to the creation of electron-hole pairs.

I. INTRODUCTION

There has been growing interest in systems with strong electron correlations and nearly half-filled bands after the discovery of the high-temperature superconductors. Undoped materials like La_2CuO_4 are Mott-Hubbard insulators, and they are well described by an isotropic spin-$\frac{1}{2}$ Heisenberg model on a square lattice. It is now believed that the spin-$\frac{1}{2}$ Heisenberg antiferromagnet in two dimensions exhibits long-range Néel order at zero temperature, although the order parameter is considerably reduced by quantum spin fluctuation. The linear spin-wave (LSW) theory[1] is known to give fairly good results for quantum corrections to various physical quantities.[2-5]

A small amount of hole doping destroys the antiferromagnet state ($x \sim 0.03$ in $La_{2-x}Sr_xCuO_4$), and eventually gives rise to a superconducting state ($x \gtrsim 0.06$). Accordingly, it is very important to study the interplay between doping and antiferromagnetism for understanding these materials. The essential aspects of the electronic structure of the CuO_2 plane may be described by a two-dimensional t-J model with the Hamiltonian given by

$$H = -t \sum_{\langle i,j \rangle,\sigma} (c_{i\sigma}^{\dagger} c_{j\sigma} + \text{H.c.}) + J \sum_{\langle i,j \rangle} \left(\mathbf{S}_i \cdot \mathbf{S}_j - \frac{n_i n_j}{4} \right) . \tag{1.1}$$

Here $\mathbf{S}_i$ is the electronic spin operator, $n_i = \sum_\sigma c_{i\sigma}^{\dagger} c_{i\sigma}$, and $\langle i,j \rangle$ refers to pairs of nearest neighbors. This model, which is derived from the large-U limit of a single-band Hubbard model,[6-9] acts on the Hilbert space with no doubly occupied sites.

The motion of a single hole in an antiferromagnetic spin background has already been studied by several authors on the basis of this model:[10-19] the motion of hole generates spin disorder, but quantum spin fluctuations repair a pair of disordered spins generated by the hole motion, leading to a coherent motion of the hole on a given sublattice. Among various approximations, the self-consistent Born approximation[13,16,17] is found to give good results for a wide range of parameter values of J/t by comparison with the results of the exact diagonalization of H for small clusters.[18,19]

For finite, nonzero dopant concentrations δ, spin waves are in return affected by the hole motion. A study of these changes is a main purpose of this paper. The local distortion of the spin configuration around static vacancies has been considered by Nagaosa, Hatsugai, and Imada[20] and Bulunt *et al.*,[21] but the effects caused by the hole motion have not been considered so far. We calculate the Green's function for holes accurate to first order in δ by extending the self-consistent Born approximation. The result is used to calculate the Green's function for spin waves by considering the creation of electron-hole pairs as well as scattering processes of spin waves by holes. Not only the coherent part but also the incoherent part of the Green's function for holes gives rise to important contributions. We find that the spin-wave velocity is strongly reduced by the presence of holes, and the reduction increases with decreasing ratios J/t. Recently Ko[22] has obtained a strong renormalization of the spin-wave velocity by considering only the scattering process of spin waves by holes, i.e., by disregarding the hopping term in Eq. (1.1). We will show that a proper account of the motion of holes decreases the contribution of the above process, thus making the process of creating electron-hole pairs more important. A strong renormalization of the spin-wave velocity has been reported in a neutron scattering experiment on $YBa_2Cu_3O_{6+x}$ by J. Rossat-Mignod *et al.*,[23] and it is probably connected with a sharp drop of the Néel temperature as a function of the dopant concentration.[24]

In Sec. II, we describe the Hamiltonian in a slave-fermion Schwinger boson representation. In Sec. III, we calculate the Green's functions for holes and spin waves, and show some numerical results. Section IV contains the concluding remarks.

II. HAMILTONIAN IN A SLAVE-FERMION SCHWINGER BOSON REPRESENTATION

We make use of a slave-fermion Schwinger boson representation $c_{i\sigma}^{\dagger} = f_i b_{i\sigma}^{\dagger}$, where the boson operator $b_{i\sigma}^{\dagger}$

keeps track of the spins, and the slave-fermion operator $f_i^\dagger$ generates a hole at site i. Although the total number of fermions and bosons on each site should be $2S$, i.e., $f_i^\dagger f_i + \sum_\sigma b_{i\sigma}^\dagger b_{i\sigma} = 2S$, we relax this constraint by using a $1/S$ expansion:[13] $b_{i\uparrow}$ as well as $b_{j\downarrow}$ are replaced by $\sqrt{2S}$ in Eq. (1.1), where the indices i and j refer to sites on the a (up) and b (down) sublattice, respectively.[25] Then the Hamiltonian is expressed as

$$H = -t\sqrt{2S}\sum_{\langle i,j\rangle}[f_i f_j^\dagger(b_{i\downarrow}^\dagger + b_{j\uparrow}) + \text{H.c.}] + J\sum_{\langle i,j\rangle} f_i f_i^\dagger f_j f_j^\dagger[-S^2 + S(b_{i\downarrow}^\dagger b_{i\downarrow} + b_{j\uparrow}^\dagger b_{j\uparrow} + b_{i\downarrow} b_{j\uparrow} + b_{i\downarrow}^\dagger b_{j\uparrow}^\dagger)] , \tag{2.1}$$

where $f_i f_i^\dagger f_j f_j^\dagger$ in the second term accounts for a loss of magnetic energy due to doping. In low concentrations, we may replace $f_i f_i^\dagger f_j f_j^\dagger = (1 - f_i^\dagger f_i)(1 - f_j^\dagger f_j)$ by $1 - f_i^\dagger f_i - f_j^\dagger f_j$. We introduce the Fourier transforms of operators in the reduced Brillouin zone (half of the first Brillouin zone),

$$f_i = \left(\frac{2}{N}\right)^{1/2}\sum_{\mathbf{k}} f_{\mathbf{k}}^a \exp(i\mathbf{k}\cdot\mathbf{r}_i) , \qquad f_j = \left(\frac{2}{N}\right)^{1/2}\sum_{\mathbf{k}} f_{\mathbf{k}}^b \exp(i\mathbf{k}\cdot\mathbf{r}_j) , \tag{2.2}$$

$$b_{i\downarrow} = \left(\frac{2}{N}\right)^{1/2}\sum_{\mathbf{k}} a_{\mathbf{k}} \exp(i\mathbf{k}\cdot\mathbf{r}_i) , \qquad b_{j\uparrow} = \left(\frac{2}{N}\right)^{1/2}\sum_{\mathbf{k}} b_{\mathbf{k}} \exp(i\mathbf{k}\cdot\mathbf{r}_j) , \tag{2.3}$$

and furthermore the Bogoliubov transformation of boson operators,

$$a_{\mathbf{k}}^\dagger = l_{\mathbf{k}}\alpha_{\mathbf{k}}^\dagger + m_{\mathbf{k}}\beta_{-\mathbf{k}}, \quad b_{-\mathbf{k}} = m_{\mathbf{k}}\alpha_{\mathbf{k}}^\dagger + l_{\mathbf{k}}\beta_{-\mathbf{k}} , \tag{2.4}$$

where

$$l_{\mathbf{k}} = \left(\frac{1+\varepsilon_{\mathbf{k}}}{2\varepsilon_{\mathbf{k}}}\right)^{1/2}, \quad m_{\mathbf{k}} = -\left(\frac{1-\varepsilon_{\mathbf{k}}}{2\varepsilon_{\mathbf{k}}}\right)^{1/2} , \tag{2.5}$$

$$\varepsilon_{\mathbf{k}} = (1-\gamma_{\mathbf{k}}^2)^{1/2}, \quad \gamma_{\mathbf{k}} = \tfrac{1}{2}(\cos k_x + \cos k_y) , \tag{2.6}$$

and N is the number of lattice sites. In the following, we consider a square lattice, and measure momenta in units of a^{-1} with a being the lattice constant. In terms of these variables we rewrite the Hamiltonian as

$$H = H_0 + H_1 + H_2 + \cdots , \tag{2.7}$$

where

$$H_0 = \sum_{\mathbf{k}} \omega_{\mathbf{k}}(\alpha_{\mathbf{k}}^\dagger\alpha_{\mathbf{k}} + \beta_{\mathbf{k}}^\dagger\beta_{\mathbf{k}}), \quad \omega_{\mathbf{k}} = JSz\varepsilon_{\mathbf{k}} , \tag{2.8}$$

$$H_1 = t\sqrt{2S}z\left(\frac{2}{N}\right)^{1/2}\sum_{\mathbf{k},\mathbf{q}} f_{\mathbf{k}-\mathbf{q}}^{b\dagger} f_{\mathbf{k}}^a \operatorname{sgn}(\gamma_{\mathbf{k}-\mathbf{q}})[(l_{\mathbf{q}}\gamma_{\mathbf{k}-\mathbf{q}} + m_{\mathbf{q}}\gamma_{\mathbf{k}})\alpha_{\mathbf{q}}^\dagger + (m_{\mathbf{q}}\gamma_{\mathbf{k}-\mathbf{q}} + l_{\mathbf{q}}\gamma_{\mathbf{k}})\beta_{-\mathbf{q}}] + \text{H.c.} , \tag{2.9}$$

$$H_2 = -JSz\frac{2}{N}\sum_{\mathbf{k},\mathbf{p},\mathbf{q}}\{f_{\mathbf{k}}^{a\dagger} f_{\mathbf{k}+\mathbf{p}-\mathbf{q}}^a[C_{\mathbf{pq}}^{(1)}\alpha_{\mathbf{p}}^\dagger\alpha_{\mathbf{q}} + C_{\mathbf{pq}}^{(2)}\beta_{\mathbf{p}}^\dagger\beta_{\mathbf{q}} + C_{\mathbf{pq}}^{(3)}(\alpha_{\mathbf{p}}^\dagger\beta_{-\mathbf{q}}^\dagger + \alpha_{-\mathbf{p}}\beta_{\mathbf{q}})] + f_{\mathbf{k}}^{b\dagger} f_{\mathbf{k}+\mathbf{p}-\mathbf{q}}^b[C_{\mathbf{pq}}^{(2)}\alpha_{\mathbf{p}}^\dagger\alpha_{\mathbf{q}} + C_{\mathbf{pq}}^{(1)}\beta_{\mathbf{p}}^\dagger\beta_{\mathbf{q}} + C_{\mathbf{qp}}^{(3)}(\alpha_{\mathbf{p}}^\dagger\beta_{-\mathbf{q}}^\dagger + \alpha_{-\mathbf{p}}\beta_{\mathbf{q}})]\} , \tag{2.10}$$

with

$$C_{\mathbf{pq}}^{(1)} = l_{\mathbf{p}}l_{\mathbf{q}} + l_{\mathbf{p}}m_{\mathbf{q}}\gamma_{\mathbf{q}} + m_{\mathbf{p}}l_{\mathbf{q}}\gamma_{\mathbf{p}} + m_{\mathbf{p}}m_{\mathbf{q}}\gamma_{\mathbf{p}-\mathbf{q}} , \tag{2.11a}$$

$$C_{\mathbf{pq}}^{(2)} = l_{\mathbf{p}}l_{\mathbf{q}}\gamma_{\mathbf{p}-\mathbf{q}} + l_{\mathbf{p}}m_{\mathbf{q}}\gamma_{\mathbf{p}} + m_{\mathbf{p}}l_{\mathbf{q}}\gamma_{\mathbf{q}} + m_{\mathbf{p}}m_{\mathbf{q}} , \tag{2.11b}$$

$$C_{\mathbf{pq}}^{(3)} = l_{\mathbf{p}}l_{\mathbf{q}}\gamma_{\mathbf{q}} + l_{\mathbf{p}}m_{\mathbf{q}} + m_{\mathbf{p}}l_{\mathbf{q}}\gamma_{\mathbf{p}-\mathbf{q}} + m_{\mathbf{p}}m_{\mathbf{q}}\gamma_{\mathbf{p}} . \tag{2.11c}$$

We have neglected unimportant terms.[26] The momentum sum is taken over the reduced Brillouin zone, and $z(=4)$ is the number of nearest neighbors. The part H_0 represents the spin-wave energy in LSW approximation, and H_1 represents the interaction between holes and spin waves. This expression for $H_0 + H_1$ has been used for studying the motion of a single hole in an antiferromagnetic spin background.[12,13,16,17] The H_2 represents the scattering of spin waves by holes. Note that $C_{\mathbf{pp}}^{(3)} = 0$.

III. GREEN'S FUNCTIONS FOR HOLES AND SPIN WAVES

Let us introduce the Green's function for holes,

$$G_{\mu\nu}(\mathbf{k},t) = -i\langle\mathcal{T}(f_{\mathbf{k}}^\mu(t)f_{\mathbf{k}}^{\nu\dagger}(0))\rangle, \quad \mu,\nu = a \text{ or } b , \tag{3.1}$$

and the Green's function for spin waves,

$$D_{\alpha\alpha}(\mathbf{k},t) = -i\langle\mathcal{T}(\alpha_{\mathbf{k}}(t)\alpha_{\mathbf{k}}^\dagger(0))\rangle , \tag{3.2a}$$

$$D_{\alpha\beta}(\mathbf{k},t) = -i\langle\mathcal{T}(\alpha_{\mathbf{k}}(t)\beta_{-\mathbf{k}}(0))\rangle , \tag{3.2b}$$

$$D_{\beta\alpha}(\mathbf{k},t) = -i\langle\mathcal{T}(\beta_{-\mathbf{k}}^\dagger(t)\alpha_{\mathbf{k}}^\dagger(0))\rangle , \tag{3.2c}$$

$$D_{\beta\beta}(\mathbf{k},t) = -i\langle\mathcal{T}(\beta_{-\mathbf{k}}^\dagger(t)\beta_{-\mathbf{k}}(0))\rangle , \tag{3.2d}$$

where $\mathcal{T}$ is the time-ordering operator, and $\langle\ \rangle$ represents an average over the ground state. Their Fourier transforms are defined by

$$G_{\mu\nu}(\mathbf{k},\omega)=\int_{-\infty}^{+\infty}dt\, G_{\mu\nu}(\mathbf{k},t)\exp(i\omega t)\ . \tag{3.3}$$

The Green's functions satisfy matrix Dyson's equations:

$$G_{\mu\nu}(\mathbf{k},\omega)= G^0_{\mu\nu}(\mathbf{k},\omega) + \sum_{\gamma\delta} G^0_{\mu\gamma}(\mathbf{k},\omega)\Sigma_{\gamma\delta}(\mathbf{k},\omega)G_{\delta\nu}(\mathbf{k},\omega)\ , \tag{3.4a}$$

$$D_{\mu\nu}(\mathbf{k},\omega)= D^0_{\mu\nu}(\mathbf{k},\omega) + \sum_{\gamma\delta} D^0_{\mu\gamma}(\mathbf{k},\omega)\Pi_{\gamma\delta}(\mathbf{k},\omega)D_{\delta\nu}(\mathbf{k},\omega)\ , \tag{3.4b}$$

where $G^0_{\mu\nu}(\mathbf{k},\omega)$ and $D^0_{\mu\nu}(\mathbf{k},\omega)$ are unperturbed Green's functions. For the antiferromagnetic ground state, the following relations hold:

$$\begin{aligned}&\Sigma_{aa}(\mathbf{k},\omega)=\Sigma_{bb}(\mathbf{k},\omega)\ ,\\ &\Sigma_{ab}(\mathbf{k},\omega)=\Sigma_{ba}(\mathbf{k},\omega)=0\ .\end{aligned} \tag{3.5}$$

In addition, since the Hamiltonian is invariant with respect to the interchanging of $(\alpha_{\mathbf{k}},f^a_{\mathbf{k}})$ and $(\beta_{\mathbf{k}},f^b_{\mathbf{k}})$, the following relations hold:

$$\begin{aligned}&\Pi_{\beta\beta}(\mathbf{k},\omega)=\Pi_{\alpha\alpha}(-\mathbf{k},-\omega)\ ,\\ &\Pi_{\beta\alpha}(\mathbf{k},\omega)=\Pi_{\alpha\beta}(-\mathbf{k},-\omega)\ .\end{aligned} \tag{3.6}$$

Note that a spiral modulation in the spin order gives rise to a nonzero off-diagonal self-energy in the Green's function for holes, i.e., $\Sigma_{ab}(\mathbf{k},\omega)\neq 0$. This leads to a splitting of the quasihole band and eventually to a stable spiral phase. For a detailed discussion on the possible spiral phase see Ref. 27. In this paper, we confine ourselves to a discussion of the Green's function for the antiferromagnetic phase. Numerical calculations are done for $S=\frac{1}{2}$.

A. The Green's function for holes

We first discuss the motion of a single hole in an antiferromagnetic background within the self-consistent Born approximation, and extend the calculation to the case of finite dopant concentrations δ by including all corrections to first order in δ.

When the problem of a single hole is considered, the unperturbed Green's functions corresponding to H_0 may be used. They are given by

$$G^0_{aa}(\mathbf{k},\omega)=G^0_{bb}(\mathbf{k},\omega)=\frac{1}{\omega+i\eta}\ , \tag{3.7a}$$

$$G^0_{ab}(\mathbf{k},\omega)=G^0_{ba}(\mathbf{k},\omega)=0\ , \tag{3.7b}$$

with $\eta=0^+$ for the hole and by

$$D^0_{\alpha\alpha}(\mathbf{q},q_0)=(q_0-\omega_{\mathbf{q}}+i\eta)^{-1}\ , \tag{3.8a}$$

$$D^0_{\alpha\beta}(\mathbf{q},q_0)=D^0_{\beta\alpha}(\mathbf{q},q_0)=0\ , \tag{3.8b}$$

$$D^0_{\beta\beta}(\mathbf{q},q_0)=(-q_0-\omega_{\mathbf{q}}+i\eta)^{-1} \tag{3.8c}$$

for the spin waves. We consider the diagram for the self-energy $\Sigma_{aa}(\mathbf{k},\omega)$ shown in Fig. 1, where the solid line represents a *dressed* Green's function $G_{bb}(\mathbf{k}-\mathbf{q},\omega-q_0)=[\omega-q_0-\Sigma_{bb}(\mathbf{k}-\mathbf{q},\omega-q_0)+i\eta]^{-1}$ and the broken line represents an unperturbed Green's function $D^0_{\alpha\alpha}(\mathbf{q},q_0)$.

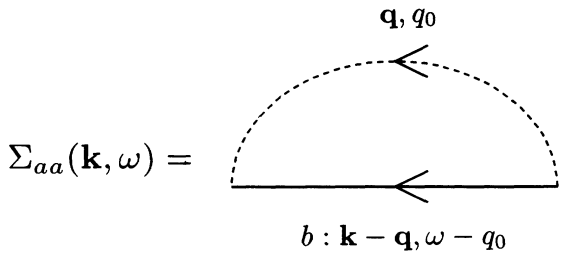

FIG. 1. Diagram for the self-energy $\Sigma_{aa}(\mathbf{k},\omega)$ in the self-consistent Born approximation. The solid line represents the dressed Green's function for holes $G_{bb}(\mathbf{k}-\mathbf{q},\omega-q_0)$. The broken line represents the unperturbed Green's function for spin waves. In finite concentrations, not only $D^0_{\alpha\alpha}(\mathbf{q},q_0)$ but also $D^0_{\beta\beta}(\mathbf{q},q_0)$ contribute to $\Sigma_{aa}(\mathbf{k},\omega)$.

This is called the self-consistent Born approximation. Explicitly the self-energy satisfies an integral equation

$$\Sigma_{aa}(\mathbf{k},\omega)= t^2z^2(2S)\frac{2}{N} \times\sum_{\mathbf{q}}\frac{M^2(\mathbf{k},\mathbf{q})}{\omega-\omega_{\mathbf{q}}-\Sigma_{aa}(\mathbf{k}-\mathbf{q},\omega-\omega_{\mathbf{q}})+i\eta}\ , \tag{3.9}$$

where $M(\mathbf{k},\mathbf{q})=l_{\mathbf{q}}\gamma_{\mathbf{k}-\mathbf{q}}+m_{\mathbf{q}}\gamma_{\mathbf{k}}$. Recently Marsiglio *et al.*[16] and Martinez and Horsch[17] have solved numerically the integral equation for a 16×16 cluster with $S=\frac{1}{2}$. We expect that vertex corrections neglected in the equation are not important, since the energy dispersion $E_{\mathbf{k}}$ of the hole which follows from the numerical solution for the self-consistent equation agrees well with the results of exact diagonalizations for small clusters in a wide range of values of J/t.[18,19] The solution has a well-defined quasihole pole due to the coherent motion and in addition a continuous incoherent spectrum, i.e.,

$$G_{aa}(\mathbf{k},\omega)=\int_{-\infty}^{+\infty}d\omega'\frac{\rho(\mathbf{k},\omega')}{\omega-\omega'+i\eta}\ , \tag{3.10a}$$

with

$$\rho(\mathbf{k},\omega)=a(\mathbf{k})\delta(\omega-E_{\mathbf{k}})+\cdots\ . \tag{3.10b}$$

The quasihole energy $E_{\mathbf{k}}$ and the residue $a(\mathbf{k})$ are given by

$$E_{\mathbf{k}}=\Sigma_{aa}(\mathbf{k},E_{\mathbf{k}}),\quad a(\mathbf{k})=\frac{1}{1-\partial\Sigma_{aa}(\mathbf{k},E_{\mathbf{k}})/\partial\omega}\ . \tag{3.11}$$

Note that $E_{\mathbf{k}}$ has minima at $\mathbf{k}_i=(\pm\pi/2,\pm\pi/2)$. In the vicinity of these minima it can be expanded as

$$E_{\mathbf{k}}=E_{\mathbf{k}_i}+\frac{1}{2m_{\parallel}}\mathbf{k}_{\parallel}^2+\frac{1}{2m_{\perp}}\mathbf{k}_{\perp}^2+\cdots\ , \tag{3.12}$$

where $\mathbf{k}_{\parallel}$ and $\mathbf{k}_{\perp}$ are the components of $\mathbf{k}-\mathbf{k}_i$ in $(1,-1)$ and $(1,1)$ directions when $\mathbf{k}_i=(\pi/2,\pi/2)$.

For finite hole concentrations, we assume that there exists a Fermi surface, inside of which the number of states equals the number of holes. In the low concentration limit, changes in the quasihole band are negligible, and therefore we define the Fermi sphere $\tilde{F}$ and the chemical potential μ by

$$\tilde{F}:\ \alpha^{-1/2}\mathbf{k}_{\parallel}^2+\alpha^{1/2}\mathbf{k}_{\perp}^2\le k_F^2\ , \tag{3.13}$$

$$\mu=E_{\mathbf{k}_i}+\frac{1}{2m}k_F^2\ , \tag{3.14}$$

where $k_F^2=\pi\delta$, $\alpha=m_{\parallel}/m_{\perp}>1$, and $m=(m_{\parallel}m_{\perp})^{1/2}$ (see Fig. 2). On the other hand, the Green's function changes through the coupling to spin waves in a complicated way to first order in δ. In order to calculate such change, we consider the self-energy given by the diagram in Fig. 1, which now turns out to consist of two terms:

$$\Sigma_{aa}(\mathbf{k},\omega)=\Sigma_{aa}^{(r)}(\mathbf{k},\omega)+\Sigma_{aa}^{(a)}(\mathbf{k},\omega)\ , \tag{3.15}$$

where the retarded part $\Sigma_{aa}^{(r)}$ arises from processes of creating an "α" spin wave in the intermediate state $[D_{\alpha\alpha}^0(\mathbf{q},q_0)]$, and the advanced part $\Sigma_{aa}^{(a)}$ arises from processes of absorbing a "β" spin wave $[D_{\beta\beta}^0(\mathbf{q},q_0)]$. Explicitly these two functions are given by

$$\Sigma_{aa}^{(r)}(\mathbf{k},\omega)=t^2z^2(2S)\frac{2}{N}\sum_{\mathbf{q}}M^2(\mathbf{k},\mathbf{q})\times\int_0^{+\infty}d\varepsilon\frac{\rho^{(+)}(\mathbf{k}-\mathbf{q},\varepsilon)}{\omega-\omega_{\mathbf{q}}-\varepsilon-\mu+i\eta}\ , \tag{3.16a}$$

$$\Sigma_{aa}^{(a)}(\mathbf{k},\omega)=t^2z^2(2S)\frac{2}{N}\sum_{\mathbf{q}}\tilde{M}^2(\mathbf{k},\mathbf{q})\times\int_{-\infty}^0 d\varepsilon\frac{\rho^{(-)}(\mathbf{k}-\mathbf{q},\varepsilon)}{\omega+\omega_{\mathbf{q}}-\varepsilon-\mu-i\eta}\ , \tag{3.16b}$$

where $\tilde{M}(\mathbf{k},\mathbf{q})=m_{\mathbf{q}}\gamma_{\mathbf{k}-\mathbf{q}}+l_{\mathbf{q}}\gamma_{\mathbf{k}}$. We have introduced the spectral representation

$$G_{aa}(\mathbf{k},\omega)=\int_0^{\infty}d\varepsilon\frac{\rho^{(+)}(\mathbf{k},\varepsilon)}{\omega-\varepsilon-\mu+i\eta}+\int_{-\infty}^0 d\varepsilon\frac{\rho^{(-)}(\mathbf{k},\varepsilon)}{\omega-\varepsilon-\mu-i\eta}\ . \tag{3.17}$$

Our aim is to calculate the Green's function for spin waves to first order in δ, and, for this purpose, we need to know $\rho^{(-)}(\mathbf{k},\varepsilon)$ to first order in δ, but we may simply use the solution $\rho(\mathbf{k},\omega)$ of the single-hole problem for $\rho^{(+)}(\mathbf{k},\varepsilon)$ by introducing the chemical potential. Neglecting irrelevant energy shifts of order δ, we evaluate $\rho^{(-)}(\mathbf{k},\varepsilon)[\equiv\rho_0^{(-)}(\mathbf{k},\varepsilon)+\rho_1^{(-)}(\mathbf{k},\varepsilon)+\cdots]$ in an iterative way as follows. First we set

$$\rho_0^{(-)}(\mathbf{k},\varepsilon)=\begin{cases}a(\mathbf{k}_i)\delta(\varepsilon+\mu-E_{\mathbf{k}_i}) & \text{for } \mathbf{k}\in\tilde{F}\ , \quad (3.18a)\\ 0 & \text{for } \mathbf{k}\notin\tilde{F}\ , \quad (3.18b)\end{cases}$$

where $\mathbf{k}_i$'s are the four wave vectors at which $E_{\mathbf{k}}$ has its minima. Next inserting Eqs. (3.18) into Eq. (3.16b), and using the relation $\rho^{(-)}(\mathbf{k},\varepsilon)=(1/\pi)\mathrm{Im}G_{aa}(\mathbf{k},\mu+\varepsilon)$, we

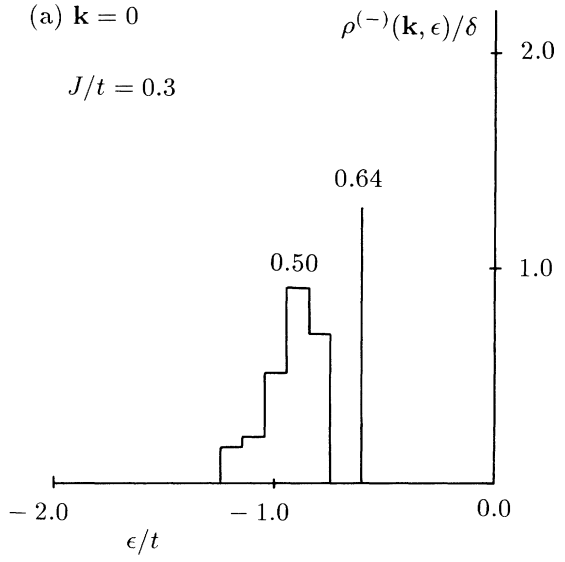

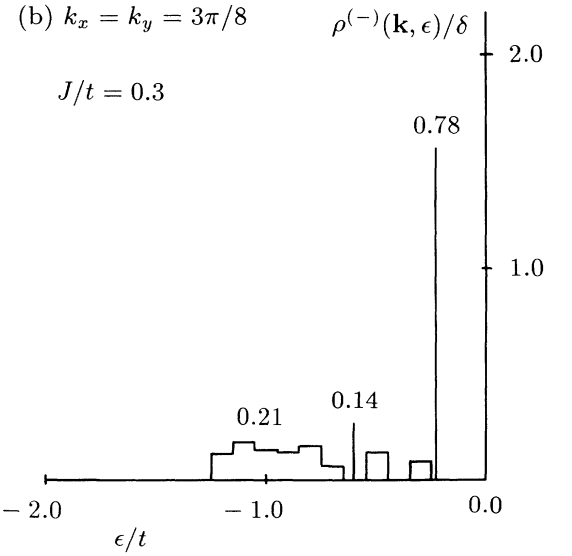

FIG. 3. $\rho_1^{(-)}(\mathbf{k},\varepsilon)/\delta$ and $\rho_2^{(-)}(\mathbf{k},\varepsilon)/\delta$ for a 16×16 cluster with $J/t=0.3$: (a) $\mathbf{k}=\mathbf{0}$, (b) $k_x=k_y=3\pi/8$. The vertical bars represent δ function of $\rho_1^{(-)}(\mathbf{k},\varepsilon)$, and the histograms represent $\rho_2^{(-)}(\mathbf{k},\varepsilon)$. The numbers attached to the δ functions and histograms represent intensities integrated with respect to ε.

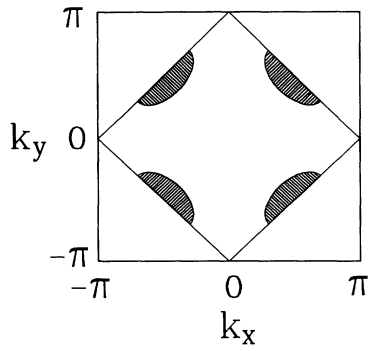

FIG. 2. Schematic plot for the Fermi surface in the reduced Brillouin zone. Regions with slanting lines represent the inside of the Fermi sphere.

obtain $\rho_1^{(-)}(\mathbf{k},\varepsilon)$ to first order in δ:

$$\rho_1^{(-)}(\mathbf{k},\varepsilon)=\frac{\delta t^2 z^2(2S)a(\mathbf{k}_i)\gamma_{\mathbf{k}}^2}{[\mu+\varepsilon-\Sigma_{aa}^{(r)}(\mathbf{k},\mu+\varepsilon)]^2}\frac{1}{4}\times\sum_i l_{\mathbf{k}_i-\mathbf{k}}^2\delta(\varepsilon+\omega_{\mathbf{k}_i-\mathbf{k}}) , \tag{3.19}$$

where the sum over i indicates an average over four hole pockets. Next inserting $\rho_1^{(-)}(\mathbf{k},\varepsilon)$ into Eq. (3.16b), we obtain

$$\rho_2^{(-)}(\mathbf{k},\varepsilon)=\frac{t^2 z^2(2S)}{[\mu+\varepsilon-\Sigma_{aa}^{(r)}(\mathbf{k},\mu+\varepsilon)]^2}\frac{2}{N}\times\sum_{\mathbf{q}}\tilde{M}^2(\mathbf{k},\mathbf{q})\int_{-\infty}^{0}d\varepsilon'\rho_1^{(-)}(\mathbf{k}-\mathbf{q},\varepsilon')\times\delta(\varepsilon+\omega_{\mathbf{q}}-\varepsilon') . \tag{3.20}$$

We obtain $\rho_3^{(-)}(\mathbf{k},\varepsilon)$ by replacing $\rho_1^{(-)}(\mathbf{k}-\mathbf{q},\varepsilon')$ in Eq. (3.20) by $\rho_2^{(-)}(\mathbf{k}-\mathbf{q},\varepsilon')$. Note that $\rho^{(-)}(\mathbf{k},\varepsilon)$ determined this way satisfies the sum rule

$$I\equiv\frac{2}{N}\sum_{\mathbf{k}}\int_{-\infty}^{0}\rho^{(-)}(\mathbf{k},\varepsilon)d\varepsilon=\delta . \tag{3.21}$$

We refer to Appendix A for the proof of Eq. (3.21). Also note that the coherent peak $\rho_0^{(-)}(\mathbf{k},\varepsilon)$ alone does not satisfy the sum rule, since $a(\mathbf{k}_i)<1$.

We solve numerically the integral equation (3.9) for a 16×16 cluster, by dividing the frequency space into meshes with their size $0.01t$ and by averaging the Green's function over each mesh size without introducing the small imaginary part to frequency. Once we obtain $\rho^{(+)}(\mathbf{k},\varepsilon)$ [or $\Sigma_{aa}^{(r)}(\mathbf{k},\varepsilon)$], we can obtain $\rho_1^{(-)}(\mathbf{k},\varepsilon)$, $\rho_2^{(-)}(\mathbf{k},\varepsilon)$, and $\rho_3^{(-)}(\mathbf{k},\varepsilon)$ by evaluating Eqs. (3.19) and (3.20). Figure 3 shows $\rho_1^{(-)}(\mathbf{k},\varepsilon)$ and $\rho_2^{(-)}(\mathbf{k},\varepsilon)$ thus evaluated for $J/t=0.3$. The iteration is rapidly convergent for $J/t\geq0.3$: I/δ evaluated up to $\rho_3^{(-)}(\mathbf{k},\varepsilon)$ is equal to 0.94 for $J/t=0.3$. [The contribution from $\rho_1^{(-)}(\mathbf{k},\varepsilon)$, $\rho_2^{(-)}(\mathbf{k},\varepsilon)$, and $\rho_3^{(-)}(\mathbf{k},\varepsilon)$ is, respectively, 0.41, 0.20, and 0.05.] The values for I/δ evaluated up to $\rho_3^{(-)}(\mathbf{k},\varepsilon)$ are shown for various values of J/t in Table I. (Several other quantities are also listed for later use.) The convergence is not rapid for $J/t=0.1$.

B. The Green's function for spin waves

We consider the diagrams shown in Fig. 4 for the self-energy of the spin-wave Green's function. Thereby the Green's functions for holes are the dressed ones evaluated in the preceding subsection. The diagrams shown in Fig. 4(a) represent the second-order processes with respect to H_1. They give rise to the self-energy

$$\Pi_{\alpha\alpha}^{(1)}(\mathbf{q},q_0)=t^2z^2(2S)\frac{2}{N}\sum_{\mathbf{k}}M^2(\mathbf{k},\mathbf{q})P_{\mathbf{k}}(\mathbf{q},q_0) , \tag{3.22a}$$

$$\Pi_{\alpha\beta}^{(1)}(\mathbf{q},q_0)=t^2z^2(2S)\frac{2}{N}\sum_{\mathbf{k}}M(\mathbf{k},\mathbf{q})\tilde{M}(\mathbf{k},\mathbf{q})P_{\mathbf{k}}(\mathbf{q},q_0) , \tag{3.22b}$$

where

$$P_{\mathbf{k}}(\mathbf{q},q_0)=\int\frac{d\omega}{2\pi i}G_{aa}(\mathbf{k},\omega)G_{bb}(\mathbf{k}-\mathbf{q},\omega-q_0)=\int_{-\infty}^{0}d\varepsilon\int_0^{\infty}d\varepsilon'\left[\frac{\rho^{(+)}(\mathbf{k},\varepsilon')\rho^{(-)}(\mathbf{k}-\mathbf{q},\varepsilon)}{q_0+\varepsilon-\varepsilon'+i\eta}-\frac{\rho^{(-)}(\mathbf{k},\varepsilon)\rho^{(+)}(\mathbf{k}-\mathbf{q},\varepsilon')}{q_0+\varepsilon'-\varepsilon-i\eta}\right] . \tag{3.23}$$

The contribution from the coherent part in Eq. (3.23) is singular and anisotropic with respect to direction of $\mathbf{q}$, as discussed before in a different context.[27] We evaluate the contribution by taking $|\mathbf{q}|\to0$ with $q_0/|\mathbf{q}|$ fixed in Eq. (3.23) with the help of the effective-mass approximation for $E_{\mathbf{k}}$ [Eq. (3.12)]. For $\mathbf{q}=(q/\sqrt{2},q/\sqrt{2})$, we obtain

$$\Pi_{\alpha\alpha}^{(1)}(\mathbf{q},q_0)=-t^2z^2(2S)[a(\mathbf{k}_i)^2 2^{-5/2}q\frac{m}{\pi}\quad\text{for } x<1 ,$$

$$=-t^2z^2(2S)[a(\mathbf{k}_i)]^2 2^{-5/2}q\frac{m}{\pi}\times\left[1-\frac{x}{(x^2-1)^{1/2}}\right]\quad\text{for } x>1 , \tag{3.24a}$$

$$\Pi_{\alpha\beta}^{(1)}(\mathbf{q},q_0)=-\Pi_{\alpha\alpha}^{(1)}(\mathbf{q},q_0) , \tag{3.24b}$$

where

$$x=\alpha^{-1/4}\frac{m}{k_F}\frac{q_0}{q} . \tag{3.25}$$

For $\mathbf{q}=(q,0)$, the same forms are obtained for the self-energy as Eqs. (3.24) but with a slightly different definition of x:

$$x=[(\alpha^{-1/2}+\alpha^{1/2})/2]^{-1/2}\frac{m}{k_F}\frac{q_0}{q} . \tag{3.26}$$

We expand Eqs. (3.24) in powers of $1/x$, and use the lead-

TABLE I. Quasihole residue $a(\mathbf{k}_i)$,[a] effective mass $m(4t)$,[a] anisotropy $\alpha\equiv m_{\parallel}/m_{\perp}$,[a] and spectral intensity I evaluated up to $\rho_3^{(-)}(\mathbf{k},\varepsilon)$.

J/t	$a(\pi/2,\pi/2)$	$m(4t)$	α	I/δ
0.10	0.13	36.0	5.3	0.85
0.30	0.28	15.3	5.9	0.94
0.50	0.39	11.6	6.1	0.98
0.80	0.50	9.9	5.5	0.98

[a]These values are equivalent to those calculated by Martinez and Horsch (Ref. 17).

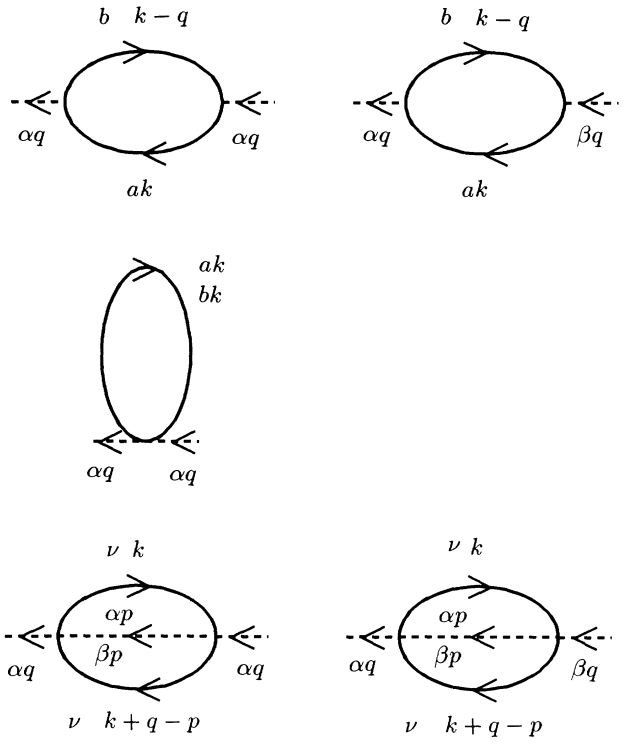

FIG. 4. Diagrams for the self-energies $\Pi^{(1)}_{\mu\nu}(\mathbf{q},q_0)$, $\Pi^{(2)}_{\mu\nu}(\mathbf{q},q_0)$, and $\Pi^{(3)}_{\mu\nu}(\mathbf{q},q_0)$. The solid lines represent the dressed Green's functions $G_{\mu\mu}(\mathbf{k},\omega)$ with $\mu=a$ or b. The broken lines represent the unperturbed Green's functions for spin waves $D^0_{\nu\nu}(\mathbf{p},p_0)$ with $\nu=\alpha$ or β.

ing term by setting $q_0=\omega_{\mathbf{q}}$, since for low hole concentrations the spin-wave velocity is much larger than that of quasiholes near the Fermi surface. As a result we obtain for the self-energy $\Pi^{(1)}_{\alpha\alpha}$ and $\mathbf{q}=(q/\sqrt{2},q/\sqrt{2})$ $(S=\frac{1}{2})$

$$\Pi^{(1)}_{\alpha\alpha}\simeq\delta\times 2\left[\frac{t}{J}\right]^3[a(\mathbf{k}_i)]^2\alpha^{1/2}\frac{1}{m^*}\omega_{\mathbf{q}}\,, \tag{3.27}$$

where $m^*=m(4t)$. For $\mathbf{q}=(q,0)$, $\alpha^{1/2}$ in Eq. (3.27) is replaced by $(\alpha^{1/2}+\alpha^{-1/2})/2$. The numerical values of $\Pi^{(1)}_{\alpha\alpha}/\delta\omega_{\mathbf{k}}$ $(\equiv A^{(1)}_{\rm coh})$ for various values of J/t are shown in Table II. Note that the self-energy $\Pi^{(1)}_{\alpha\alpha}$ is positive. The situation differs from the one encountered in the electron-phonon problem where the sound velocity is smaller than the velocity of electrons at the Fermi surface.

On the other hand, the other contributions to $\Pi^{(1)}_{\alpha\alpha}$ are not singular for $\mathbf{q}\to\mathbf{0}$, $q_0\to 0$. Since the matrix elements $M^2(\mathbf{k},\mathbf{q})$ and $M(\mathbf{k},\mathbf{q})\tilde{M}(\mathbf{k},\mathbf{q})$ are proportional to $|\mathbf{q}|$ for small $\mathbf{q}$ (see Appendix B), we may replace $\rho^{(\pm)}(\mathbf{k}-\mathbf{q},\varepsilon)$ by $\rho^{(\pm)}(\mathbf{k},\varepsilon)$, and set $q_0=0$ in the denominator of Eq. (3.23) in order to pick up terms to lowest order for small wave vector $\mathbf{q}$. In the numerical evaluation of Eq. (3.23), we assume that only $\mathbf{k}=\mathbf{k}_i$ is inside the Fermi sphere among the discrete values of $\mathbf{k}$, and take account of $\rho^{(-)}(\mathbf{k},\varepsilon)$ up to $\rho^{(-)}_3(\mathbf{k},\varepsilon)$. The numerical values of $\Pi^{(1)}_{\alpha\alpha}/\delta\omega_{\mathbf{k}}$ $(\equiv A^{(1)}_{\rm inc})$ thus evaluated are shown in Table II for various values of J/t. They are negative, and their absolute values increase with decreasing ratios J/t.

The diagram in Fig. 4(b) represents the first-order processes with respect to H_2, and gives rise to the self-energy

$$\Pi^{(2)}_{\alpha\alpha}(\mathbf{q},q_0)=-JSz\frac{2}{N}\sum_{\mathbf{k}}\int_{-\infty}^{\infty}\frac{d\omega}{2\pi}ie^{i\omega\eta}[\,C^{(1)}_{\mathbf{qq}}G_{aa}(\mathbf{k},\omega)+C^{(2)}_{\mathbf{qq}}G_{bb}(\mathbf{k},\omega)]$$
$$=-2\delta\omega_{\mathbf{q}}\,, \tag{3.28a}$$

$$\Pi^{(2)}_{\alpha\beta}(\mathbf{q},q_0)=0\,. \tag{3.28b}$$

Equation (3.28b) results from $C^{(3)}_{\mathbf{qq}}=0$. The diagrams in Fig. 4(c) represent the second-order processes with respect to H_2, and contribute to the self-energy

$$\Pi^{(3)}_{\alpha\alpha}(\mathbf{q},q_0)=(JSz)^2\left[\frac{2}{N}\right]^2\sum_{\mathbf{k},\mathbf{p}}\int_{-\infty}^{0}d\varepsilon\int_0^{\infty}d\varepsilon'\left\{(|C^{(1)}_{\mathbf{qp}}|^2+|C^{(2)}_{\mathbf{qp}}|^2)\frac{\rho^{(+)}(\mathbf{k}+\mathbf{q}-\mathbf{p},\varepsilon')\rho^{(-)}(\mathbf{k},\varepsilon)}{q_0+\varepsilon-\varepsilon'-\omega_{\mathbf{p}}+i\eta}\right.$$
$$\left.-(|C^{(3)}_{\mathbf{qp}}|^2+|C^{(3)}_{\mathbf{pq}}|^2)\frac{\rho^{(-)}(\mathbf{k}+\mathbf{q}-\mathbf{p},\varepsilon)\rho^{(+)}(\mathbf{k},\varepsilon')}{q_0+\varepsilon'-\varepsilon+\omega_{\mathbf{p}}-i\eta}\right\}, \tag{3.29a}$$

TABLE II. Self-energies divided by $\delta\omega_{\mathbf{q}}$ for small $\mathbf{q}$ in (1,1) and (1,0) directions: $A^{(i)}\equiv\Pi^{(i)}_{\alpha\alpha}/\delta\omega_{\mathbf{q}}$. The values $A^{(1)}_{\rm inc}$, $A^{(2)}$, and $A^{(3)}$ are independent of direction of $\mathbf{q}$.

J/t		$A^{(1)}_{\rm coh}$ [a]	$A^{(1)}_{\rm inc}$	$A^{(2)}$	$A^{(3)}$	Total
0.10	(1,1)	2.19	−28.99	−2	−0.12	−28.92
	(1,0)	1.30				−29.81
0.30	(1,1)	0.95	−8.14	−2	−0.30	−9.49
	(1,0)	0.55				−9.89
0.50	(1,1)	0.51	−4.21	−2	−0.46	−6.16
	(1,0)	0.30				−6.37
0.80	(1,1)	0.24	−1.97	−2	−0.62	−4.35
	(1,0)	0.14				−4.45

[a]Values evaluated from Eq. (3.27).

$$\Pi^{(3)}_{\alpha\beta}(\mathbf{q},q_0)=(JSz)^2\left[\frac{2}{N}\right]^2\sum_{\mathbf{k},\mathbf{p}}\int_{-\infty}^{0}d\varepsilon\int_{0}^{\infty}d\varepsilon'(C^{(1)}_{\mathbf{qp}}C^{(3)}_{\mathbf{pq}}+C^{(2)}_{\mathbf{qp}}C^{(3)}_{\mathbf{qp}})$$
$$\times\left[\frac{\rho^{(+)}(\mathbf{k}+\mathbf{q}-\mathbf{p},\varepsilon')\rho^{(-)}(\mathbf{k},\varepsilon)}{q_0+\varepsilon-\varepsilon'-\omega_{\mathbf{p}}+i\eta}-\frac{\rho^{(-)}(\mathbf{k}+\mathbf{q}-\mathbf{p},\varepsilon)\rho^{(+)}(\mathbf{k},\varepsilon')}{q_0+\varepsilon'-\varepsilon+\omega_{\mathbf{p}}-i\eta}\right]. \quad (3.29b)$$

Since the matrix elements $C^{(i)}_{\mathbf{qp}}$ are proportional to $|\mathbf{q}|^{1/2}$ for small $|\mathbf{q}|$ (see Appendix B), we replace $\rho^{(\pm)}(\mathbf{k}+\mathbf{q}-\mathbf{p},\varepsilon)$ by $\rho^{(\pm)}(\mathbf{k}-\mathbf{p},\varepsilon)$, and set $q_0=0$ in the denominators in Eqs. (3.29) in order to pick up terms of lowest order for small $\mathbf{q}$. The numerical values of $\Pi^{(3)}_{\alpha\alpha}/\delta\omega_{\mathbf{k}}$ ($\equiv A^{(3)}$) thus evaluated are shown in Table II for various values of J/t. They are negative, and their absolute values increase with increasing ratios J/t, but are much smaller than $A^{(1)}_{\text{inc}}$.

Since the self-energy for small $\mathbf{q}$ is expressed as $\Pi_{\alpha\alpha}=\Pi_{\beta\beta}=A\delta\omega_{\mathbf{q}}$, $\Pi_{\alpha\beta}=\Pi_{\beta\alpha}=B\delta\omega_{\mathbf{q}}$, the Green's function is given by

$$D^{-1}(\mathbf{q},q_0)=\begin{bmatrix}q_0-(1+A\delta)\omega_{\mathbf{q}} & -B\delta\omega_{\mathbf{q}}\\ -B\delta\omega_{\mathbf{q}} & -q_0-(1+A\delta)\omega_{\mathbf{q}}\end{bmatrix}. \quad (3.30)$$

The renormalized spin-wave energy $\tilde{\omega}_{\mathbf{q}}$ is determined from the condition $\det D(\mathbf{q},\tilde{\omega}_{\mathbf{q}})^{-1}=0$ and therefore given by

$$\tilde{\omega}_{\mathbf{q}}=[(1+A\delta)^2-B^2\delta^2]^{1/2}\omega_{\mathbf{q}}\simeq(1+A\delta)\omega_{\mathbf{q}}. \quad (3.31)$$

By using the values for A listed in Table II we can determine the critical dopant concentration δ_c at which the spin-wave velocity becomes zero. We expect that for $\delta>\delta_c$ (for example, $\simeq 0.11$ at $J/t=0.3$) antiferromagnetism is destroyed by the holes.

IV. CONCLUDING REMARKS

We have studied the renormalization of spin waves for low dopant concentrations δ in the t-J model, by using a large-S approximation to the slave-fermion Schwinger boson representation. We have calculated the Green's function for holes to first order in δ, on the basis of the self-consistent Born approximation. We expect that this procedure works well at low dopant concentrations in view of its success in describing the motion of a single hole.[16,17] With the help of this result, we have calculated the self-energy for the spin-wave Green's function by taking account of the processes in which electron-hole pairs are created and spin waves are scattered by holes. The incoherent part of the Green's function for holes gives rise to important contributions to the self-energy. The spin-wave velocity is found to be strongly renormalized by the former process, and the reduction rate increases with decreasing ratios J/t. The strong renormalization with $J/t\to 0$ suggests the instability of the antiferromagnetism in this limit, and reminds us of Nagaoka's ferromagnetic state.[28] Our result is qualitatively in agreement with neutron scattering experiments.[23]

In this paper, we have assumed an antiferromagnetic spin configuration. As was discussed by Shraiman and Siggia,[29] Eder,[30] and the present authors,[27] no matter how small the dopant concentration is, the antiferromagnetic state is always unstable against formation of a spiral. The discussions in this paper can be applied to the spiral phase with a slight modification, leading to a renormalization of the spin-wave velocity.[31] The doping dependence of the stiffness constant and related problems are presently also under investigation by applying projection techniques.[32] The results obtained so far are similar to ours.

Note added in proof. A value of the same order of magnitude as δ_c was also obtained in Ref. 33.

ACKNOWLEDGMENTS

We would like to thank Professor K. W. Becker, Dr. R. Eder, Dr. P. Horsch, and U. Muschelknautz for helpful discussions.

APPENDIX A: PROOF OF A SUM RULE

Let I_i be

$$I_i=\frac{2}{N}\sum_{\mathbf{k}}\int_{-\infty}^{0}d\varepsilon\,\rho_i^{(-)}(\mathbf{k},\varepsilon). \quad (A1)$$

Substituting Eqs. (3.18)–(3.20) into Eq. (A1), we obtain

$$I_0=\delta a(\mathbf{k}_i), \quad (A2)$$

$$I_1=\delta a(\mathbf{k}_i)t^2z^2(2S)\frac{2}{N}\times\sum_{\mathbf{k}}\frac{\gamma^2_{\mathbf{k}}I^2_{\mathbf{k}_i-\mathbf{k}}}{[\mu-\omega_{\mathbf{k}_i-\mathbf{k}}-\Sigma^{(r)}_{aa}(\mathbf{k}_i,\mu-\omega_{\mathbf{k}_i-\mathbf{k}})]^2}, \quad (A3)$$

and so on. On the other hand, since the retarded part of the self-energy satisfies Eq. (3.9), its derivative must satisfy a relation

$$\frac{\partial}{\partial\omega}\Sigma^{(r)}_{aa}(\mathbf{k},\omega)|_{\omega=\mu}=t^2z^2(2S)\frac{2}{N}\sum_{\mathbf{q}}\frac{-M^2(\mathbf{k},\mathbf{q})[1-\partial\Sigma^{(r)}_{aa}(\mathbf{k}-\mathbf{q},\omega-\omega_{\mathbf{q}})/\partial\omega|_{\omega=\mu}]}{[\mu-\omega_{\mathbf{q}}-\Sigma^{(r)}_{aa}(\mathbf{k}-\mathbf{q},\mu-\omega_{\mathbf{q}})]^2}. \quad (A4)$$

We notice that the first term in Eq. (A4) for $\mathbf{k}=\mathbf{k}_i$ is equal to $-I_1/[\delta a(\mathbf{k}_i)]$. Applying a similar procedure to the derivative of the self-energy in the second term of Eq. (A4), we obtain a term equivalent to $-I_2/[\delta a(\mathbf{k}_i)]$. In this way we can prove the following relation step by step:

$$I_0+I_1+I_2+\cdots=\delta a(\mathbf{k}_i)[1-\partial\Sigma(\mathbf{k}_i,\omega)/\partial\omega|_{\omega=\mu}] =\delta \ . \tag{A5}$$

APPENDIX B: MATRIX ELEMENTS FOR SMALL MOMENTUM

We summarize the matrix elements expanded for small $\mathbf{q}$:

$$C^{(1)}_{\mathbf{pq}}=C^{(1)}_{\mathbf{qp}}\simeq B_1(\mathbf{p})q^{1/2}-m_{\mathrm{p}}\Delta(\mathbf{p},\mathbf{q}) \ , \tag{B1}$$

$$C^{(2)}_{\mathbf{pq}}=C^{(2)}_{\mathbf{qp}}\simeq B_2(\mathbf{p})q^{1/2}+l_{\mathrm{p}}\Delta(\mathbf{p},\mathbf{q}) \ , \tag{B2}$$

$$C^{(3)}_{\mathbf{pq}}\simeq B_1(\mathbf{p})q^{1/2}+m_{\mathrm{p}}\Delta(\mathbf{p},\mathbf{q}) \ , \tag{B3}$$

$$C^{(3)}_{\mathbf{qp}}\simeq B_2(\mathbf{p})q^{1/2}-l_{\mathrm{p}}\Delta(\mathbf{p},\mathbf{q}) \ , \tag{B4}$$

$$M(\mathbf{k},\mathbf{q})\simeq 2^{-3/4}q^{1/2}\gamma_{\mathbf{k}}+\Delta(\mathbf{k},\mathbf{q}) \ , \tag{B5}$$

$$\tilde{M}(\mathbf{k},\mathbf{q})\simeq 2^{-3/4}q^{1/2}\gamma_{\mathbf{k}}-\Delta(\mathbf{k},\mathbf{q}) \ , \tag{B6}$$

where

$$B_1(\mathbf{p})=(l_{\mathrm{p}}+m_{\mathrm{p}}\gamma_{\mathrm{p}})/2^{3/4} \ , \quad B_2(\mathbf{p})=(l_{\mathrm{p}}\gamma_{\mathrm{p}}+m_{\mathrm{p}})/2^{3/4} \ , \tag{B7}$$

$$\Delta(\mathbf{p},\mathbf{q})=(q_x\sin p_x+q_y\sin p_y)/(2^{5/4}q^{1/2}) \ . \tag{B8}$$

[1] P. W. Anderson, Phys. Rev. **86**, 694 (1952); R. Kubo, *ibid.* **87**, 568 (1952).

[2] P. Horsch and W. von der Linden, Z. Phys. B **72**, 181 (1988).

[3] K. W. Becker, H. Won, and P. Fulde, Z. Phys. B **75**, 335 (1988).

[4] R. R. P. Singh and D. A. Huse, Phys. Rev. B **40**, 7247 (1989).

[5] J. Igarashi and A. Watabe, Phys. Rev. B **43**, 13 456 (1991); **44**, 5054 (1991).

[6] P. W. Anderson, Science **235**, 1196 (1987); Phys. Rep. **184**, 195 (1989).

[7] V. J. Emery, Phys. Rev. Lett. **58**, 2794 (1987).

[8] F. C. Zhang and T. M. Rice, Phys. Rev. B **37**, 3759 (1988).

[9] H. Eskes and G. A. Sawatzky, Phys. Rev. Lett. **61**, 1415 (1988).

[10] L. N. Bulaevskii, E. L. Nagaev, and D. L. Khomskii, Zh. Eksp. Teor. Fiz. **54**, 1562 (1968) [Sov. Phys. JETP **27**, 1562 (1968)].

[11] W. F. Brinkman and T. M. Rice, Phys. Rev. B **2**, 1324 (1970); B. I. Shraiman and E. D. Siggia, Phys. Rev. Lett. **60**, 740 (1988).

[12] S. Schmitt-Rink, C. M. Varma, and A. E. Ruckenstein, Phys. Rev. Lett. **60**, 2793 (1988).

[13] C. L. Kane, P. A. Lee, and N. Read, Phys. Rev. B **39**, 6880 (1989).

[14] R. Eder and K. W. Becker, Z. Phys. B **78**, 219 (1990); R. Eder, K. W. Becker, and W. Stephan, *ibid.* **81**, 33 (1990).

[15] S. A. Trugman, Phys. Rev. B **37**, 1597 (1988); **41**, 892 (1990); J. Inoue and S. Maekawa, J. Phys. Soc. Jpn. **59**, 2110 (1989).

[16] F. Marsiglio, A. E. Ruckenstein, S. Schmitt-Rink, and C. M. Varma, Phys. Rev. B **43**, 10 882 (1991).

[17] G. Martinez and P. Horsch, Phys. Rev. B **44**, 317 (1991).

[18] K. J. von Szczepanski, P. Horsch, W. Stephan, and M. Ziegler, Phys. Rev. B **41**, 2017 (1990).

[19] E. Dagotto, R. Joynt, A. Moreo, S. Bacci, and E. Gagliano, Phys. Rev. B **41**, 9049 (1990).

[20] N. Nagaosa, Y. Hatsugai, and M. Imada, J. Phys. Soc. Jpn. **59**, 978 (1989).

[21] N. Bulunt, D. Hone, D. J. Scalapino, and E. Y. Loh, Phys. Rev. Lett. **62**, 2192 (1989).

[22] D. Y. K. Ko, Phys. Rev. Lett. **65**, 116 (1990).

[23] J. Rossat-Mignod, J. X. Boucherle, P. Burlet, J. Y. Henry, J. M. Jurgens, G. Lapertot, L. P. Regnault, J. Schweizer, F. Tasset, and C. Vettier, in *Proceedings of the International Seminar on High-T_c Superconductors, Dubna, 1989,* edited by V. L. Aksenov, N. N. Bogoliubov, and N. M. Plakida (World Scientific, Singapore, 1990), p. 74.

[24] R. J. Birgeneau and G. Shirane, in *Physical Properties of High Temperature Superconductors,* edited by D. M. Ginsburg (World Scientific, Singapore, 1989).

[25] Using the constraint condition, we replace $S^z_i=f_i f^\dagger_i(b^\dagger_{i\uparrow}b_{i\uparrow}-b^\dagger_{i\downarrow}b_{i\downarrow})$ by $S^z_i=f_i f^\dagger_i(2S-2b^\dagger_{i\downarrow}b_{i\downarrow}-f^\dagger_i f_i)=f_i f^\dagger_i(2S-b^\dagger_{i\downarrow}b_{i\downarrow})$.

[26] Neglected terms in Eq. (2.7) are $-(N/2)JS^2z+JSz\sum_{\mathbf{k}}(\varepsilon_{\mathbf{k}}-1)+(JS^2z-JSz\varepsilon_{\mathrm{av}})\sum_{\mathbf{k}}(f^{a\dagger}_{\mathbf{k}}f^a_{\mathbf{k}}+f^{b\dagger}_{\mathbf{k}}f^b_{\mathbf{k}})$, with $\varepsilon_{\mathrm{av}}=(2/N)\sum_{\mathrm{p}}(\varepsilon_{\mathrm{p}}-1)$. These terms give rise to only a constant shift to the excitation energy of hole.

[27] J. Igarashi and P. Fulde, Phys. Rev. B **45**, 10 419 (1992).

[28] Y. Nagaoka, Phys. Rev. **147**, 392 (1966).

[29] B. I. Shraiman and E. D. Siggia, Phys. Rev. Lett. **61**, 467 (1988); **62**, 1564 (1989).

[30] R. Eder, Phys. Rev. B **43**, 10 706 (1991).

[31] There appears a strongly hybridized mode which is characterized for the spiral phase, as discussed in Ref. 27.

[32] U. Muschelknautz and K. W. Becker (unpublished).

[33] G. G. Khaliullin, Pis'ma Zh. Eksp. Teor. Fiz. **52**, 999 (1990) [JETP Lett. **52**, 389 (1991)].